

ANALYSIS AND CHARACTERIZATION OF COMPLEX SPATIO-TEMPORAL PATTERNS IN NONLINEAR REACTION-DIFFUSION SYSTEMS

Nita Parekh, V. Ravi Kumar, and B.D. Kulkarni*
Chemical Engineering Division,
National Chemical Laboratory,
Pune - 411 008, INDIA

Abstract

Two important classes of spatio-temporal patterns, namely, spatio-temporal chaos and self-replicating patterns, for a representative three variable autocatalytic reaction mechanism coupled with diffusion has been studied. The characterization of these patterns has been carried out in terms of Lyapunov exponents and dimension density. The results show a linear scaling as a function of sub-system size for the Lyapunov dimension and entropy while the Lyapunov dimension density was found to rapidly saturate. The possibility of synchronizing the spatio-temporal dynamics by analyzing the conditional Lyapunov exponents of sub-systems was also observed.

Keywords: Spatio-temporal chaos; self-replication; reaction-diffusion; autocatalysis; Lyapunov exponents; synchronization

1 Introduction

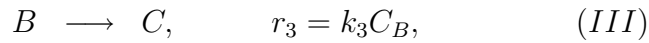
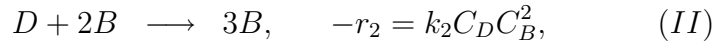
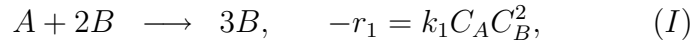
The study of temporal chaos – based on the analysis of data from physical measurements at a point in phase-space or using model equations defined as a set of ordinary differential equations (ODE's) – has matured considerably. Thus, methods for characterizing the basic properties of low-dimensional nonlinear systems are now reasonably well developed [1,2]. In comparison, the understanding of spatio-temporal chaos is at a less developed level and presently considerable attention is being focussed on this topic [1,2,3]. Examples of systems exhibiting complex spatio-temporal patterns include hydrodynamic systems [4,5], thermal convection in fluids [6], nonlinear optics [7], chemical reactions [8,9], excitable biological systems [10], crystallization and solidification fronts [11], etc. The phenomenological models in the form of nonlinear partial differential equations (PDEs), e.g., the Swift-Hohenberg equation and its variants, the Kuramoto-Sivashinsky equation, Ginzburg-Landau equation and reaction-diffusion models have been developed to study the nonlinear and nonequilibrium properties of these systems [2]. Other modelling strategies such as Coupled Map Lattices (CMLs) [12], Cellular Automata (CA) [13], lattice gas models and their derivatives [14] have also been used for understanding the dynamical behavior of the spatially-extended systems. These methods have been successfully employed for analyzing multi-phase flow systems, reaction-diffusion behavior, polymeric dynamics, etc.

For the phase-space reconstruction and model building of the spatio-temporal systems, attempts have been made to generalize the known methods of analyzing temporal systems from time-series data [1]. For higher dimensional systems, the analysis turns out to be computationally very demanding because of the large number of spatial degrees of freedom [15-18]. In this paper, we aim at exemplifying some features of sub-system behavior which may help in the characterization of the spatio-temporal behavior of reaction-diffusion systems exhibiting complex dynamics. We shall focus attention on quantitatively estimating the degree of space-time coherence in the apparently complex

dynamics (e.g., spatio-temporal chaos and self-replicating patterns) that arise in a representative nonlinear autocatalytic reaction model. Our analysis gives interesting relationships in the system invariant properties as a function of sub-system size. We have also attempted to study the dynamical synchronization properties of this extended system from sub-system analysis. The possibility of synchronizing the behavior of spatio-temporal dynamics may have considerable implications in the control of the system behavior.

2 Model Development

The objectives outlined above were studied by considering a specific example from a fairly general class of mechanisms in chemically reacting systems and commonly referred to in the literature as an autocatalator [19,20]. The reaction scheme considered here is the three-step parallel autocatalytic reaction mechanism [20] with competing interactions between the chemical species A , D , and B and expressed as,



with the rate expression r_i , $i = 1, 2, 3$ for each step given alongside. As may be seen nonlinear feedback occurs due to the rates of formation of species B being autocatalytic in steps I and II while in III the effect is counteractive and inhibitory. For a continuous flow well-mixed cell, the model description for the above reaction mechanism takes the following dimensionless form

$$\begin{aligned} \frac{dX_1}{dt} &= 1 - X_1 - Da_1 X_1 X_3^2 \\ \frac{dX_2}{dt} &= \beta - X_2 - Da_2 X_2 X_3^2 \\ \frac{dX_3}{dt} &= 1 - (1 + Da_3) X_3 + \alpha (Da_1 X_1 + Da_2 X_2) X_3^2, \end{aligned} \quad (1)$$

where X_i , $i = 1, 2, 3$, respectively, represent the dimensionless species concentrations of A , D , and B relative to their concentrations at the inlet to the

cell from the surroundings. Here, Da_i 's are dimensionless kinetic parameters associated with the reaction steps (I-III) and the parameters α and β are the feed concentration ratios of species B and D with respect to A . An analysis of the bifurcation map and dynamics of this cell is known to exhibit features such as multistationarity, oscillations and low dimensional chaos in system parameter space of α , β and Da_i 's [20]. The corresponding model for a diffusion mechanism operating in one spatial dimension x may be written as

$$\begin{aligned}
\frac{\partial X_1(x,t)}{\partial t} &= 1 - X_1(x,t) - Da_1 X_1(x,t) X_3^2(x,t) + d_1 \frac{\partial^2 X_1(x,t)}{\partial x^2} \\
\frac{\partial X_2(x,t)}{\partial t} &= \beta - X_2(x,t) - Da_2 X_2(x,t) X_3^2(x,t) + d_2 \frac{\partial^2 X_2(x,t)}{\partial x^2} \\
\frac{\partial X_3(x,t)}{\partial t} &= 1 - (1 + Da_3) X_3(x,t) + \alpha [Da_1 X_1(x,t) + Da_2 X_2(x,t)] X_3^2(x,t) \\
&\quad + d_3 \frac{\partial^2 X_3(x,t)}{\partial x^2}, \tag{2}
\end{aligned}$$

where d_i , $i = 1, 2, 3$ are the diffusion coefficients of the species A , D , and B respectively. The Euler discretization of the Laplacian yields

$$\begin{aligned}
\frac{\partial X_1(j,t)}{\partial t} &= 1 - X_1(j,t) - Da_1 X_1(j,t) X_3^2(j,t) \\
&\quad + D_1 [X_1(j+1,t) - 2X_1(j,t) + X_1(j-1,t)] \\
\frac{\partial X_2(j,t)}{\partial t} &= \beta - X_2(j,t) - Da_2 X_2(j,t) X_3^2(j,t) \\
&\quad + D_2 [X_2(j+1,t) - 2X_2(j,t) + X_2(j-1,t)] \\
\frac{\partial X_3(j,t)}{\partial t} &= 1 - (1 + Da_3) X_3(j,t) + \alpha [Da_1 X_1(j,t) + Da_2 X_2(j,t)] X_3^2(j,t) \\
&\quad + D_3 [X_3(j+1,t) - 2X_3(j,t) + X_3(j-1,t)], \tag{3}
\end{aligned}$$

$D_i = d_i/(\Delta x)^2$; Δx is the spatial mesh size of the discretized lattice; and $j = 1, 2, \dots, N$. This discretized model may be considered to describe the dynamics of N autocatalytic cells defined by (1) and coupled through diffusion. The effects of diffusion may result in an interplay between the local cell dynamics and this in turn may lead to pattern formation. The number of degrees of freedom is now significantly increased to $3N$ and the characterization of the system dynamics is not a trivial task. Here, the diffusion coefficients of species A and D are assumed equal and much greater than for species B , i.e., $D_1 = D_2 > D_3$. This is in accordance with Turing's conjecture for the occurrence of spatio-temporal patterns in biological systems [21]. It has been shown

that for appropriate choices of diffusion rates, a variety of stationary spatio-temporal patterns such as target, striped, or hexagonal patterns and travelling waves may develop in simple reaction-diffusion systems [22,23]. Recently, this conjecture has been confirmed by experiments with thin two-dimensional gel laboratory reactors uncontaminated by convection effects [24,25].

For the first part of the study all the cells of the system were assigned identical initial conditions and the parameter values were chosen corresponding to single cell (1) exhibiting chaotic dynamics. The chaotic nature of the single cell dynamics was confirmed by the positive value of the maximum Lyapunov exponent for its temporal dynamics, $\lambda_{max} \sim 1.36$. The extended system (3) dynamics was then simulated using the fourth order Runge-Kutta algorithm with time step $\Delta t = 0.0002$. The studies were carried out on a one-dimensional lattice with $N = 64$ and periodic boundary conditions were given. In fig. 1, for time $t < 40$ in dimensionless units, the system dynamics is seen to be spatially correlated though temporally it is uncorrelated and chaotic. Note that the diffusion mechanism is not active in this region because of identical initial conditions assumed over the entire spatial domain, i.e., all the cells evolve in phase with each other. Now at time $t = 40$, a perturbation was given to the chosen eleven cells lying in the central region of the lattice. This perturbation assumed that the dynamics of the chosen cells progressively went out of phase with each other by time $t = 0.002$. A spread of this perturbation to the system boundaries by diffusion, with a simultaneous loss in the spatial correlation, is qualitatively seen in fig. 1. This loss in the spatial correlation was seen to persist even at $t = 10,000$ time units (results not presented here).

In the second part of this study we considered the system in the parameter range where it might exhibit coherent patterns and one such interesting pattern is shown in fig. 2. In this case, the perturbation was seen to develop into peaks that self-replicate structurally in time. Similar patterns have been observed in a two-variable model system [26,27]. Recent experiments have also shown their presence unambiguously [25]. This self-replicating behavior, is in a sense, analogous to what is observed during the phenomenon of self-replicating

growth of biological cells [28], DNA and RNA [29,30], micelles [31], etc. For comparative purposes, it may be noted that for the study in fig.2, the mathematical model for the three step autocatalytic reaction mechanism, assumed the form similar to that considered in [27] by suitable dimensionalization. i.e.,

$$\begin{aligned}
\frac{\partial X_1(x,t)}{\partial t} &= 1 - X_1(x,t) - Da_1 X_1(x,t) X_3^2(x,t) + d_1 \frac{\partial^2 X_1(x,t)}{\partial x^2} \\
\frac{\partial X_2(x,t)}{\partial t} &= \beta - X_2(x,t) - Da_2 X_2(x,t) X_3^2(x,t) + d_2 \frac{\partial^2 X_2(x,t)}{\partial x^2} \\
\frac{\partial X_3(x,t)}{\partial t} &= - (1 + Da_3) X_3(x,t) + \alpha [Da_1 X_1(x,t) + Da_2 X_2(x,t)] X_3^2(x,t) \\
&\quad + d_3 \frac{\partial^2 X_3(x,t)}{\partial x^2},
\end{aligned} \tag{4}$$

We shall study the dynamical characterization of the above two widely different and important class of spatio-temporal patterns, namely, (a) the chaotic behavior and (b) the coherent self-replicating behavior.

3 Characterization of Spatio-Temporal Dynamics

We shall first discuss the characterization of chaotic dynamics exhibited by this spatially extended system in terms of the system Lyapunov exponents [32]. For the present system with three species interacting on a one-dimensional lattice of size N there exists $3N$ Lyapunov exponents and their calculation is computationally very demanding. To alleviate this problem we propose to analyze the Lyapunov spectrum of its sub-systems of size $n_s (< N)$ as $n_s \rightarrow N$ and look for any interesting relationships that may help in characterizing the system dynamics. We shall now briefly discuss below the calculation of sub-system Lyapunov exponents.

For the extended system (3) with κ denoting the set of fixed parameters, the temporal evolution of the concentrations of each of the species for chosen

values of D_i may be functionally written as

$$\frac{dX_i(k, t)}{dt} = F_{i,k}(X_i(k, t), X_i(k \pm 1, t), D_i, \kappa), \quad (5)$$

where the first index $i = 1, 2, 3$ denotes the respective species and the second index $k = 1, \dots, n_s$ denotes a sub-system lattice site. For a sub-system of size n_s , there are $3n_s$ independent variables and therefore $3n_s$ exponents. These may be calculated by monitoring the growth rate of $3n_s$ sets of orthonormal vectors $\delta X_i(k, t)$, $i = 1, 2, 3$, $k = 1, 2, \dots, n_s$, in a linearized region of (3). The complete set of linearized equations built around a reference system state $\mathbf{X}_r(t) \equiv X_i(k, t)$ may then be written as

$$\frac{d\delta\mathbf{X}(t)}{dt} = \mathbf{J}\delta\mathbf{X}(t). \quad (6)$$

Here, \mathbf{J} is the augmented Jacobian of size $3n_s \times 3n_s$ evaluated at $\mathbf{X}_r(t)$ and $\delta\mathbf{X}(t)$ refers to the infinitesimal perturbation from this reference state. Using the fundamental matrix $\phi(t, t_0)$ the $3n_s$ solutions of (6) may be expressed in a general form as

$$\delta\mathbf{X}(t) = \phi(t, t_0)\delta\mathbf{X}(t_0). \quad (7)$$

The above relation is a linear map of different vector spaces. That is, $\phi(t, t_0)$ is the mapping of $\delta\mathbf{X}(t_0)$ (related to the tangent space E_0 at the phase-space point $\mathbf{X}_r(t_0) = X_i(k, t_0)$) to $\delta\mathbf{X}(t)$ (associated with the tangent space E_t for the phase-space point $\mathbf{X}_r(t) = X_i(k, t)$) with

$$\phi(t, t_0) = \phi(t, t_{n-1}) \dots \phi(t_2, t_1)\phi(t_1, t_0). \quad (8)$$

The time averaging of $\delta\mathbf{X}(t)$, along with Gram-Schmidt orthonormalization at periodic intervals, yields the $3n_s$ sub-system Lyapunov exponents as

$$\lambda_j^{(s)} = \lim_{t \rightarrow \infty} \sup \frac{1}{t} \ln \frac{|\delta\mathbf{X}(t)|}{|\delta\mathbf{X}(t_0)|}, \quad j = 1 \dots 3n_s, \quad (9)$$

in a decreasing order. While calculating these exponents for the discrete set of equations (3), fixed boundary conditions were assumed at the sub-system boundary sites, i.e., at $k = 1$ and $k = n_s$. The fixed boundary conditions suggest that only for the purposes of evaluating the λ_j , the flow of information from the outer site of the sub-system boundaries, may be likened, to presence of noise in the analysis.

Using the above formalism we found that convergence of the sub-system Lyapunov exponents was robust, although, for large n_s the computer time required was extremely high. In figs. 3a and 3b is shown the channelled dynamics, considered from the central region in fig. 1, for sub-systems $n_s = 7$ and $n_s = 31$, respectively. The convergence behavior of the maximum sub-system exponent for these cases is presented in figs. 3c and 3d.

For the analysis of the complete system dynamics we consider the Kaplan and Yorke conjecture [32,33] to calculate the effective sub-system Lyapunov dimension $d_L^{(s)}$ defined as

$$d_L^{(s)} = j + \frac{1}{|\lambda_{j+1}^{(s)}|} \sum_{i=1}^j \lambda_i^{(s)}, \quad (10)$$

where j is the largest integer for which the sum of the exponents, $\lambda_1^{(s)} + \dots + \lambda_j^{(s)} \geq 0$. In fig. 4a is shown a plot of the sub-system dimension $d_L^{(s)}$ as a function of its size n_s . A clear linear scaling relationship in the sub-system dimension is seen with its size, indicating that analysis of relatively small sized sub-systems may suffice in estimating the effective dimensionality of the large system. It may be noted that similar interesting relationships in Lyapunov dimensions as a function of lattice system size have been observed in coupled maps [18] indicating a possible generalization. Further, for analyzing the spatial complexities in the system dynamics we studied the behavior of sub-system dimension density function $\rho^{(s)}$ defined as

$$\rho^{(s)} = \lim_{n_s \rightarrow \infty} \frac{d_L^{(s)}}{n_s}. \quad (11)$$

A plot of $\rho^{(s)}$ as a function of sub-system size n_s in fig. 4b depicts a rapid convergence to a constant value (~ 0.57 for $n_s > n_{sc}$) although the entropy (defined as the sum of the sub-system positive Lyapunov exponents) increases linearly with n_s (fig. 4c). This increase in entropy suggests that the rate of information production and the growth of uncertainty varies with the sub-system size. Further, the converging behavior of $\rho^{(s)}$ may help in assessing the complexity in the system dynamics. On comparing the magnitudes of $\rho^{(s)}$ for the case without diffusion to that when diffusion is present, we find that there is

marked drop in its value from 2.01 (without diffusion) to 0.57 (with diffusion). This implies that diffusion results in a decrease in the average contribution to the Lyapunov dimension from each cell and attempts to bring about spatial uniformity in the system variables. The sensitive nonlinear features however play an antagonistic role. In summary, a knowledge of the Lyapunov dimension $d_L^{(s)}$ and the corresponding dimension density $\rho^{(s)}$ of a sub-system can help in resolving the extents of complexity in the system dynamics.

We also studied the effect of varying the diffusion coefficients of the interacting species (but maintaining their ratio constant) on the system dynamics. In fig. 5 are shown plots of D_1 as a function of dimension density $\rho^{(s)}$ (for $n_s = 7$) for two different ratios of D_3/D_1 . The figure shows the region where the spatio-temporal behavior is more sensitive to the values of the diffusion coefficients and points out that the chaotic patterns may break into coherent ones (at $D_1 = 0.75$). It may be clarified that similar behavior may also be observed for variations in the other system parameters.

The characterization studies of coherent but self-replicating patterns shown in fig. 2 yield a negative maximum Lyapunov exponent ($\lambda_{max} \sim -0.07$, calculated for $n_s = 21$). Thus, although the dynamics of these patterns are complex, the negative value suggests that the pattern would finally evolve to a stationary system solution.

4 Synchronization of Spatio-Temporal Dynamics

In this section, we shall analyze the capability of a suitably chosen response system to synchronize its dynamics with that of a spatio-temporal chaotic system using limited time-series data. In the context of low-dimensional chaotic dynamics it has been observed that synchronization is possible if conditional Lyapunov exponents turn out to be negative [34,35]. The results obtained in

Section 3 suggest that it may be worthwhile to study whether it is sufficient to calculate the conditional Lyapunov exponents for the sub-system of the response model to determine its synchronizing ability. Note that the response model has a reduced dimensionality because it is driven by space-time signals in one of the dependent variables X_i , $i = 1, 2$, or 3 . We shall present the results on assuming that space-time data in $X_3(j, t)$ are available. The model of the response system then assumes the form

$$\begin{aligned} \frac{\partial \hat{X}_1(j, t)}{\partial t} &= 1 - \hat{X}_1(j, t) - Da_1 \hat{X}_1(j, t) X_3^2(j, t) \\ &\quad + D_1 [\hat{X}_1(j+1, t) - 2\hat{X}_1(j, t) + \hat{X}_1(j-1, t)] \\ \frac{\partial \hat{X}_2(j, t)}{\partial t} &= \beta - \hat{X}_2(j, t) - Da_2 \hat{X}_2(j, t) X_3^2(j, t) \\ &\quad + D_2 [\hat{X}_2(j+1, t) - 2\hat{X}_2(j, t) + \hat{X}_2(j-1, t)], \end{aligned} \quad (12)$$

where $\hat{X}_1(j, t)$ and $\hat{X}_2(j, t)$, $j = 1, 2, \dots, N$ are the response variables.

Similar to the sub-system Lyapunov exponents, it is possible to calculate the conditional sub-system exponents by monitoring the growth rate of now $2n_s$ sets of orthonormal vectors $\delta X_i(k, t)$, $i = 1, 2$, $k = 1, 2, \dots, n_s$ in a linearized region of (12) but in the reduced dimensionality index i .

We found the maximum conditional sub-system exponent (for the chaotic dynamics in fig. 1 with $n_s = 11$) to be negative indicating that the response system may have the ability to synchronize. This was tested by dynamically passing space-time signals in the variables $X_3(j, t)$ ($j = 1, \dots, N$) from (3) to the response system defined by (12) (for $N = 64$). For the study it was further assumed that the response system did not experience the finite amplitude perturbation and was only temporally chaotic, while, (3) had evolved considerably into spatio-temporal chaos before time-series signals in $X_3(j, t)$ were passed to (12). The simulation showed that the dynamics of the response system did synchronize completely with the main system. This is depicted in figs. 6a and 6b where the space-time errors converge to zero over the entire spatial domain in both the dependent variables $e_i(t) = X_i(j, t) - \hat{X}_i(j, t)$, ($i = 1, 2$).

For the self-replicating patterns (fig. 2), the maximum sub-system exponent calculated from (3) was found to be negative as reported above. The evaluation of the conditional exponents is trivial and synchronization is again likely to occur. From a different perspective, we have in an alternate study, focussed our attention on the synchronization behavior of these patterns with a view to controlling the dynamics of this interesting class of spatio-temporal patterns [36].

5 Conclusions

In summary, the characterization of a reaction-diffusion system with nonlinear autocatalytic kinetics and exhibiting complex dynamics has been studied from a viewpoint of relating spatial sub-system dynamical behavior to that of the system considered as a whole. The analysis indicates that for the system exhibiting spatio-temporal chaos there exists a linear scaling relationship in the Lyapunov dimension $d_L^{(s)}$ as the sub-system size n_s increases. For a set of operating parameter values it is also seen that above a critical sub-system size n_{sc} , the Lyapunov density function $\rho^{(s)}(= d_L^{(s)}/n_s)$, which quantifies the average information, saturates to a constant value. The growth of uncertainty of the system and rate of information production evaluated in terms of the K-S entropy, however, increases linearly with sub-system size. These results may help in formulating strategies for embedding complex dynamics of reaction-diffusion systems from time-series data.

Apart from chaotic spatio-temporal patterns this system is also seen to exhibit other interesting patterns for suitable choices of parameter values. One such interesting pattern, viz., the self-replicating patterns, has been demonstrated. The sensitivity of the complex dynamics to operating values and especially the magnitudes of the diffusion coefficient has been brought out. Finally, the synchronization ability of the dynamics of a response system using time-series data from the spatial domain was analyzed for both spatio-

temporally chaotic and self-replicating dynamics. Our analysis indicates that if the maximum conditional Lyapunov exponent of a sub-system is negative, synchronization over the entire spatial domain is likely to occur.

Acknowledgements We gratefully acknowledge the support of the Department of Science and Technology, New Delhi, India, in carrying out this work.

References

- [1] H.D.I. Abarbanel, R. Brown, J.J. Sidorowich and Lev Sh. Tsimring, *Rev. Mod. Phys.* 65 (1993) 1331.
- [2] M.C. Cross and P. C. Hohenberg, *Rev. Mod. Phys.* 65 (1993) 851.
- [3] Hie-Tae Moon, *Rev. Mod. Phys.* 65 (1993) 1535.
- [4] W. Barten, M. Lücke, W. Hort and M. Kamps, *Phys. Rev. Lett.* 63 (1989) 376.
- [5] V. Steinberg and E. Kaplan, *Spontaneous Formation of Space-time Structures and Criticality*, ed. T. Riste and D. Sherrington (Plenum, N.Y., 1991) p207.
- [6] A.C. Newell, T. Passot and J. Lega, *Annu. Rev. Fluid Mech.* 25 (1993) 399.
- [7] J.V. Moloney and A.C. Newell, *Nonlinear Optics* (Addison Wesley, Reading, MA, 1992).
- [8] A.T. Winfree, *Chaos* 1 (1991) 303.
- [9] G. Nicolis, *J. Phys. Condens. Matter* 2 (1990) SA47.
- [10] A.J. Koch and H. Meinhardt, *Rev. Mod. Phys.* 66 (1994) 1481.
- [11] J.M. Flesselles, A.J. Simon and A. Libchaber, *Adv. Phys.* 40 (1991) 1.
- [12] K. Kaneko, *Physica D* 34 (1989) 1.
- [13] S. Wolfram, Ed., *Theory and Applications of Cellular Automata* (World Scientific, Singapore, 1986)
- [14] D. Gary, D. Doolen, ed., *Lattice Gas Methods for Partial Differential Equations* (Addison Wesley Publ. Co., 1990).
- [15] P. Grassberger, *Phys. Scr.* 40 (1989) 346.
- [16] G. Mayer-Kress and K. Kaneko, *J. Stat. Phys.* 54 (1989) 1489.

- [17] A. Torcini, A. Politi, G. Puccioni and G. Alessandro, *Physica D* 53 (1991) 85.
- [18] M. Bauer, H. Heng and W. Martienssen, *Phys. Rev. Lett.* 71 (1993) 521.
- [19] P. Gray and S. Scott, *Chem. Eng. Sci.* 38 (1983) 29.
- [20] D.T. Lynch, *Chem. Eng. Sci.* 47 (1992) 4435.
- [21] A.M. Turing, *Phil. Trans. Roy. Soc. B* 327 (1952) 37.
- [22] V. Castets, E. Dulos, J. Boissonade and P. De Kepper, *Phys. Rev. Lett.* 64 (1990) 2953.
- [23] Q. Ouyang and H. L. Swinney, *Nature* 352 (1991) 610.
- [24] K.J. Lee, W. D. McCormick, Q. Ouyang and H. L. Swinney, *Science* 261 (1993) 192.
- [25] K.J. Lee, W. D. McCormick, J. E. Pearson and H. L. Swinney, *Nature* 369 (1994) 215.
- [26] J. E. Pearson, *Science* 261 (1993) 189.
- [27] W. N. Reynolds, J. E. Pearson and S. Ponce-Dawson, *Phys. Rev. Lett.* 72 (1994) 2797.
- [28] J.D. Murray, *Mathematical Biology* (Springer, New York, 1989)
- [29] W.C. Gardiner, *Biologically Inspired Physics*, ed. L. Peliti, (Plenum Press, New York, 1991) p317.
- [30] W. Banzhaf, *Biological Cybernetics* 69 (1993) 269.
- [31] A.P. Bachmann, P. L. Luisi and J. Lang, *Nature* 357 (1992) 57.
- [32] J. Argyris, G. Faust, M. Haase, *An Exploration of Chaos* (Elsevier Science B.V., Amsterdam, 1994).
- [33] J.L. Kaplan, J.A. Yorke, *Lecture Notes in Mathematics*, 730 1979 204.
- [34] L.M. Pecora and T. L. Carroll, *Phys. Rev. A.* 44 (1991) 2374.

- [35] M. Ding and E. Ott, Phys. Rev. E. 49, R945 (1994).
- [36] N. Parekh, V. Ravi Kumar and B.D. Kulkarni, Phys. Rev. E., in press (1995).

Figure 1:

Spatio-temporal chaos arising for a perturbation given at $T = 40$. $D_1 = D_2 = 1.0$; $D_3 = 0.01$; $\alpha = 1.5$; $\beta = 2.93$; $Da_1 = 18000$; $Da_2 = 400$; $Da_3 = 80$; [X_1 axis-scale: (0.0, 0.07); x axis-scale: (0.0, 12.8); t axis-scale: (0.0, 100.0)].

Figure 2:

Self-replicating pattern for the three-variable autocatalytic reaction $D_1 = D_2 = 1.0$; $D_3 = 0.01$; $\alpha = 1.0$; $\beta = 1.0$; $Da_1 = 50$; $Da_2 = 50$; $Da_3 = 2.95$; For the entire system (with $N = 256$) placed in a homogeneous stationary state [$X_1(0, 0) = 1.0$, $X_2(0, 0) = 1.0$, $X_3(x, 0) = 0.0$] at $t = 0$, a finite perturbation $X_1(0, 0) = 0.5$, $X_2(0, 0) = 0.5$, $X_3(x, 0) = 0.25$ was given in the central 21 sites. [X_3 axis-scale: (0.0, 2.96); x axis-scale: (0.0, 51.2) ; t axis-scale: (0.0, 200.0)].

Figure 3:

Sub-system dynamics for spatio-temporal chaos (a) $n_s = 7$; (b) $n_s = 21$. (c,d) The respective convergence of the maximum Lyapunov exponent for the above sub-systems. System parameter values and other conditions of analysis identical to fig. 1.

Figure 4:

Behavior of sub-system a) Lyapunov dimension, b) dimension density, and c) entropy as a function of n_s .

Figure 5:

Sensitivity of dimension density $\rho^{(s)}$ for varying D_1 for two different ratios of D_3/D_1 ($D_2 = D_1$). Solid curve: $D_3/D_1 = 0.01$; dashed curve: $D_3/D_1 = 0.1$.

Figure 6:

Space-time errors converging to zero in both the dependent variables, $e_i(t) = X_i(j, t) - \hat{X}_i(j, t)$, $j = 1, \dots, N$ (a) $i = 1$, (b) $i = 2$ indicative of complete synchronization in the spatio-temporal chaotic dynamics of the system and its response model. System parameter values and other conditions of analysis identical to fig. 1. Note the response model had initial conditions (corresponding to temporal chaos) while the system had developed into spatio-temporal chaos (i.e. 100 time units in Fig. 1) at $t = 0$ when driving was switched on. X_1 axis-scale: (a) (-24, 26), (b) (-45, 9.5); x axis-scale: (0.0, 51.2); t axis-scale: (0.0, 200.0).